



# Real-time monitoring of cell surface protein arrival with split luciferases

Alexandra A. M. Fischer<sup>1,2,3</sup>  | Larissa Schatz<sup>4,5</sup> | Julia Baaske<sup>1,2</sup> |  
Winfried Römer<sup>1,2</sup> | Wilfried Weber<sup>1,2,3,6,7</sup> | Roland Thuenauer<sup>4,5,8</sup> 

<sup>1</sup>Signaling Research Centres BIOSS and CIBSS and Faculty of Biology, University of Freiburg, Freiburg, Germany

<sup>2</sup>Faculty of Biology, University of Freiburg, Freiburg, Germany

<sup>3</sup>Spemann Graduate School of Biology and Medicine (SGBM), University of Freiburg, Freiburg, Germany

<sup>4</sup>Centre for Structural Systems Biology (CSSB), Hamburg, Germany

<sup>5</sup>Technology Platform Light Microscopy, University of Hamburg, Hamburg, Germany

<sup>6</sup>INM – Leibniz Institute for New Materials, Saarbrücken, Germany

<sup>7</sup>Department of Materials Science and Engineering, Saarland University, Saarbrücken, Germany

<sup>8</sup>Technology Platform Microscopy and Image Analysis (TP MIA), Leibniz Institute of Virology (LIV), Hamburg, Germany

## Correspondence

Roland Thuenauer, Centre for Structural Systems Biology (CSSB), Hamburg, Germany.  
Email: [roland.thuenauer@cssb-hamburg.de](mailto:roland.thuenauer@cssb-hamburg.de)

## Funding information

Deutsche Forschungsgemeinschaft; Ministry of Science, Research and the Arts of Baden-Württemberg

## Abstract

Each cell in a multicellular organism permanently adjusts the concentration of its cell surface proteins. In particular, epithelial cells tightly control the number of carriers, transporters and cell adhesion proteins at their plasma membrane. However, sensitively measuring the cell surface concentration of a particular protein of interest in live cells and in real time represents a considerable challenge. Here, we introduce a novel approach based on split luciferases, which uses one luciferase fragment as a tag on the protein of interest and the second fragment as a supplement to the extracellular medium. Once the protein of interest arrives at the cell surface, the luciferase fragments complement and generate luminescence. We compared the performance of split Gaussia luciferase and split Nanoluciferase by using a system to synchronize biosynthetic trafficking with conditional aggregation domains. The best results were achieved with split Nanoluciferase, for which luminescence increased more than 6000-fold upon recombination. Furthermore, we showed that our approach can separately detect and quantify the arrival of membrane proteins at the apical and basolateral plasma membrane in single polarized epithelial cells by detecting the luminescence signals with a microscope, thus opening novel avenues for characterizing the variations in trafficking in individual epithelial cells.

## KEYWORDS

apical membrane traffic, basolateral membrane traffic, cell polarization, epithelial cells, protein sorting, Split luciferases

## 1 | INTRODUCTION

The cell surface concentration of membrane proteins, such as receptors or cell adhesion proteins, determines how a cell communicates and interacts with its environment and thus ensures the proper function of a cell within a multicellular organism. The localization of membrane proteins at the plasma membrane is regulated by biosynthetic, endocytic, recycling and degradative trafficking pathways, which

enable the cell to adjust the cell surface concentration of specific proteins on a timescale of seconds to minutes.<sup>1–3</sup>

Exact monitoring of changes in the cell surface concentration of a membrane protein of interest (POI) in live cells in real-time represents a considerable challenge. Direct quantification with fluorescence microscopy is currently not achievable, because whole live cells would have to be repeatedly imaged with a spatial resolution of <5 nm to reliably discern proteins in the plasma membrane from proteins that are still at the

This is an open access article under the terms of the [Creative Commons Attribution-NonCommercial-NoDerivs](https://creativecommons.org/licenses/by-nc-nd/4.0/) License, which permits use and distribution in any medium, provided the original work is properly cited, the use is non-commercial and no modifications or adaptations are made.

© 2023 The Authors. *Traffic* published by John Wiley & Sons Ltd.

cytoplasm, for example, in endosomes adjacent to the plasma membrane. An approach to resolve this “resolution problem” are membrane impermeant labels for the POI, which specifically bind and therefore label proteins at the cell surface when applied to the extracellular medium. For example, the addition of fluorescently labeled antibodies, which bind to the extracellular domain of the POI, represents a commonly used strategy to measure the plasma membrane concentration of proteins in flow cytometry<sup>4</sup> and can also be adapted for adherent cells.<sup>5</sup> Nevertheless, when applying fluorescently labeled antibodies to the extracellular medium, considerable background signal from unbound antibodies prevents a precise and sensitive measurement of the signal from bound antibodies. To avoid this, unbound antibodies can be removed by additional washing steps, which, however, precludes real-time monitoring.

To avoid washing steps, a probe is required that only produces a signal when bound to the POI. An ideal probe for measuring rapid changes in cell surface concentrations of proteins needs to fulfill certain conditions: (1) Signal levels should increase significantly upon binding, ideally by several orders of magnitude, to enable sensitive detection and limiting the required probe concentration. (2) Signals should be generated rapidly after binding, ideally within <1 min, to follow rapid changes in cell surface protein concentration. It is worth noting that rapid and stable signal generation upon binding benefits from high on-rates ( $k_{on}$ ) of the probe and low dissociation constants ( $k_d$ ). Two different types of approaches for generating signals only upon cell surface arrival of proteins have been developed. The first type is based on fluorogenic probes, which increase their fluorescence when bound, and the second type is based on split reporters, which only generate signals upon recombination of the split reporter fragments. Nevertheless, all approaches reported so far have limitations, and none simultaneously meets conditions (1) and (2) as defined before. This allowed to utilize them only for specific applications: For example, membrane-impermeable fluorogenic probes that can be specifically attached to proteins of interest via SNAP and HALO tags have been recently developed.<sup>6</sup> However, SNAP-based probes have a rather low  $k_{on}$  in the range of  $10^3 \text{ M}^{-1} \text{ s}^{-1}$ ,<sup>7</sup> which means that very high concentrations of the probe have to be used and fast kinetic changes cannot be properly monitored. HALO-based probes do have 1000–10 000 times higher  $k_{on}$  values, but available probes do show only a six-fold increase of fluorescence signal levels upon binding,<sup>6</sup> which results in comparably high background signals from unbound probes, thus limiting the sensitivity of the assay. Split GFP variants represent the best-studied split reporters that have been utilized for measuring the cell surface concentration of proteins.<sup>8</sup> However, recombined split GFPs need typically >15 min to become fully fluorescent.<sup>9,10</sup> This slow kinetics makes it impossible to use split GFPs for measuring changes in cell surface protein concentrations in real-time.

Here, we adapt split luciferases for measuring the cell surface concentration of membrane proteins in real-time. We tested split *Gussia* luciferase (GLuc)<sup>11</sup> and split Nanoluciferase<sup>12</sup> for real-time monitoring of the cell surface arrival of membrane proteins that were synchronously released from the ER using a conditional aggregation domain (CAD)-based system.<sup>13</sup> Recombined split Nanoluciferase yielded much higher signals and was therefore characterized further.

Luminescence was detectable within <1 min after recombination of split Nanoluciferase and luminescence levels increased more than 6000-fold upon recombination. The split Nanoluciferase has superior kinetics and signal-increase properties. Furthermore, a small tag of only 11 amino acids needs to be added to the POI, which is available as variants with  $k_d$  values ranging from  $10^{-5} \text{ M}$  to  $10^{-10} \text{ M}$ .<sup>12</sup> All that makes this system a powerful and versatile tool for monitoring cell surface concentrations of proteins in real-time. To demonstrate the capabilities of the system we show real-time measurements of cell surface arrival in single cells via microscopy and specific measurements of apical and basolateral arrival in polarized epithelial cells.

## 2 | RESULTS

### 2.1 | Functional principle of split luciferase-mediated detection of cell surface arrival and construct design

To control protein trafficking to the plasma membrane, we used the previously established CAD-system that enables synchronizing secretory protein trafficking.<sup>13</sup> The construct (pCMV-CAD4-FCS-HA-POI-mCherry, Figure 1A) consists of four CADs that retain the POI in the endoplasmic reticulum (ER) after synthesis by aggregate formation. Adding the small molecule D/D-Solubilizer dissolves the aggregates and leads to the release of POIs from the ER in a synchronized wave. If desired, cycloheximide can be added together with D/D-Solubilizer to prevent further protein synthesis during release. Once the POIs reach the Golgi apparatus, the protease furin, which is located mainly at the trans-Golgi network, cleaves at the furin cleavage site (FCS) and POIs without their CAD-tags are trafficked to the plasma membrane. After insertion into the plasma membrane, they expose the HA-tag to the extracellular space. This system has been characterized before for measuring the cell surface concentration of proteins with extracellularly applied antibodies (Figure 1A,B).<sup>5,13</sup> Here, we added a split luciferase fragment to the construct (pCMV-CAD4-FCS-Split\_Luc-HA-POI-mCherry) that is also extracellularly exposed after protein insertion into the plasma membrane. The respective other split luciferase fragment was produced recombinantly in *Escherichia coli* and added extracellularly. Thereby, the arrival of the proteins at the plasma membrane could be detected in real-time by recombination of both fragments. Mardin Darby canine kidney (MDCK) cells were used because they readily form epithelial monolayers.<sup>3,14,15</sup> Rhodopsin (rhod)<sup>13</sup> and p75<sup>16</sup> were used as markers for apical protein trafficking and the neural cell adhesion molecule (NCAM)<sup>17</sup> as basolateral marker.

### 2.2 | System development and characterization

In our initial approach, we tested the detection of proteins arriving at the cell surface using the *Gussia* luciferase and one of its mutants called “Monsta.” We split *Gussia* luciferase between Gly93 and Glu94 and named them NGLuc and CGLuc, respectively.<sup>11</sup> Then, we

**FIGURE 1** Construct design and mode of function of the split luciferase real-time reporter for protein plasma membrane arrival. (A) Construct for synchronized protein trafficking (“CAD-System”) consisting of a signal sequence (SS) for ER targeting, four conditional aggregation domains (CADs), a furin cleavage site (FCS), a split luciferase fragment (Split\_Luc), HA-tag, the protein of interest (POI) and mCherry. POIs lacking the four CADs (lower construct) insert into the plasma membrane independent of D/D-Solubilizer addition. (B) POIs are first retained in the ER because of aggregation of the CADs. The addition of the D/D-Solubilizer dissolves these aggregates, and POIs traffic to the trans-Golgi network where the protease furin is located. Furin cleaves at the FCS and POIs without CAD tags progress to the plasma membrane. After insertion of the POI into the plasma membrane, the fused Split\_Luc fragment and the HA-tag are exposed to the extracellular space and bind the recombinantly produced second Split\_Luc fragment.

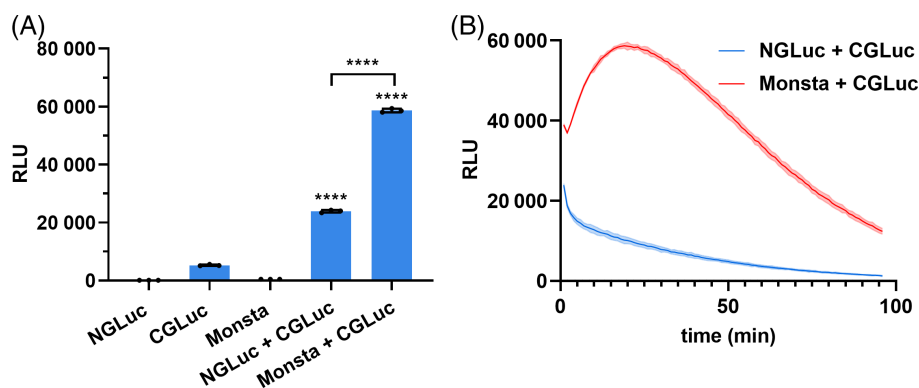
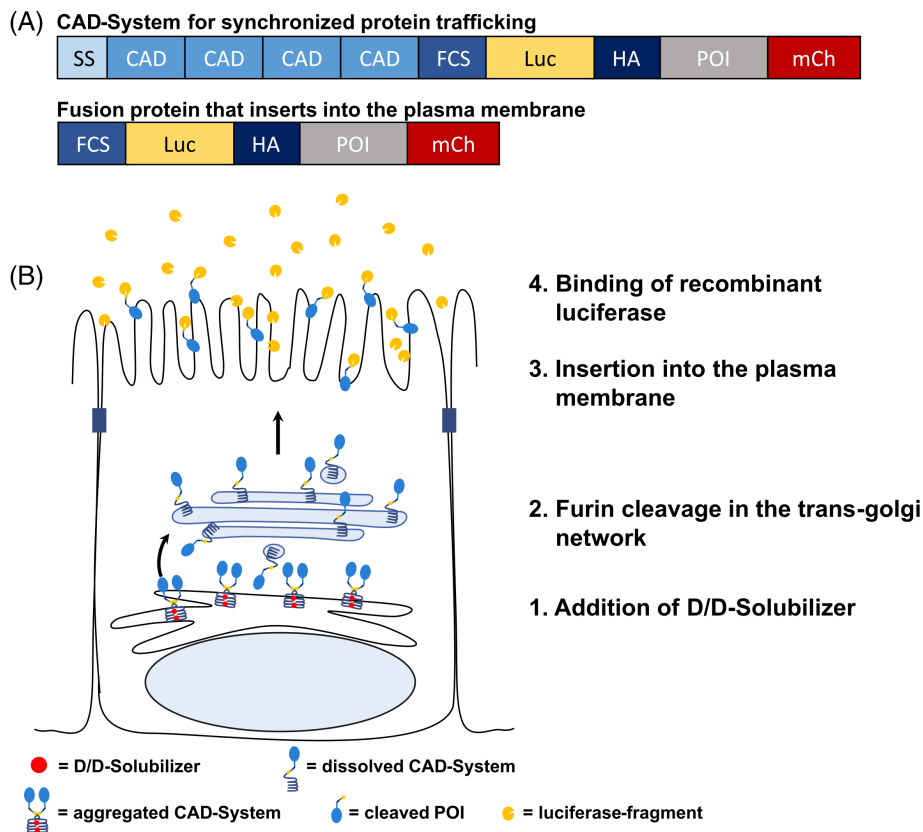


**FIGURE 2** The activity of recombinantly produced split Gaussia luciferase fragments. (A) Indicated GLuc fragments were combined in 1:1 ratio at 1.25  $\mu$ M concentration and luminescence in relative light units (RLU) was detected, maximum values of each time course are plotted,  $p$  values were calculated with a Student's  $t$  test (\*\*\*\* $p < 0.001$ ). (B) Distinct luminous behavior of wild-type GLuc and Monsta mutant over time. Fragments were combined in 1:1 ratio at 1.25  $\mu$ M concentration, signals were measured every minute.

inserted four point mutations in the N-terminus to create the Monsta variant, which is brighter and exhibits glow-type luminescence in comparison to the flash-type kinetics of wild-type Gaussia luciferase.<sup>18</sup> We produced the three luciferase fragments in *E. coli* and tested their functionality by mixing the eluates. The combination of NGLuc and CGLuc led to significantly increased luminescence values and the exchange of NGLuc by Monsta further increased the signal 2.4-fold. Single NGLuc and Monsta did not have activity alone, whereas CGLuc had low intrinsic activity at high concentrations (Figure 2A). We assumed that this activity was because of homooligomerization of

CGLuc (Figure S1A). As expected, wild-type Gaussia exhibited flash-type kinetics, whereas Monsta had higher and prolonged glow-type kinetics (Figure 2B). Due to the low yield in CGLuc protein production (Figure S1A), and to avoid background signal generation from homooligomers of purified CGLuc, we decided to fuse CGLuc to our POIs (CGLuc-HA-POI-mCherry). For testing, we produced stable cell lines that express CGLuc-POI at the plasma membrane. We could only detect small quantities of CGLuc-p75 and CGLuc-NCAM at the plasma membrane, and CGLuc-rhod was not detectable at all (Figure S1B). We concluded that neither wild-type nor Monsta GLuc was sensitive

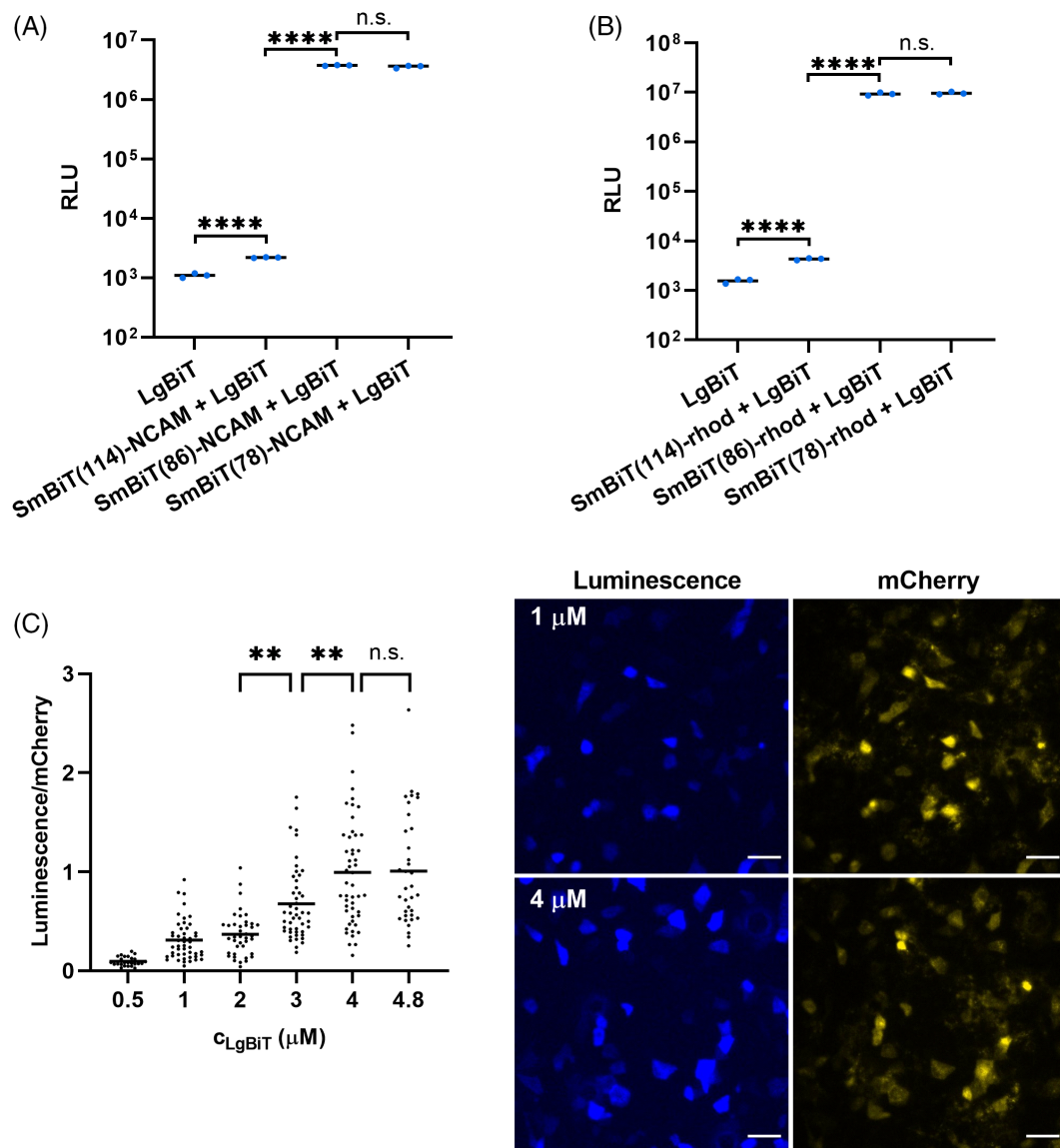


**FIGURE 3** Detection of NCAM and rhod at the plasma membrane using split Nanoluciferase. (A,B) NCAM or rhod fused to the indicated SmBiT variant were transfected into unpolarized MDCK cells 12 h prior to the measurement. LgBiT was added at 83.3 nM concentration and substrate was used in 1:300 dilution. LgBiT in the extracellular medium showed a low intrinsic background activity, which is even detectable in untransfected cells. Mean values of triplicates  $\pm$  SD are plotted.  $p$  values were calculated with a Student's  $t$  test (n.s.  $p > 0.05$ ; \*\*\*\* $p < 0.001$ ). (C) Detection of rhod at the cell surface via microscopy. Unpolarized MDCK cells were transfected with SmBiT(86)-rhod and LgBiT was added at the indicated concentrations. Luminescence and mCherry images of  $N > 25$  cells were acquired with a confocal microscope using a 20 $\times$  objective, scale bars indicate 50  $\mu$ m. For quantitative analysis (left) background signals were subtracted and luminescence values were normalized to the mCherry signal of each cell. An outlier analysis was performed using GraphPad Prism (ROUT method,  $Q = 0.1\%$ ). Means with individual values ( $N > 25$ ) are plotted and an ordinary one-way ANOVA with multiple comparisons was performed (n.s.  $p > 0.05$ ; \*\* $p < 0.01$ ), images of representative cells are shown (right).

enough to detect low protein amounts at the plasma membrane. Furthermore, microscopy showed that for CGLuc-tagged p75, NCAM and rhod, a considerable amount was retained intracellularly after 3 h of release (Figure S2), which indicates a problem with proper POI trafficking to the plasma membrane.

Therefore, we decided to test the NanoBiTs<sup>®</sup> system based on the Nanoluciferase for our purposes. Nanoluciferase is smaller, brighter and more stable compared to other luciferases and its split

version is dissected asymmetrically into an 18 kDa, N-terminal part (LgBiT) and a 1.3 kDa, C-terminal part (SmBiT). The SmBiT is available with different affinities to the LgBiT. Therefore, we chose the SmBiT that was optimized for protein-protein interaction studies (SmBiT(114),  $K_D = 1.9 \times 10^{-4}$ ) and two high affinity variants: SmBiT(86) ( $K_D = 0.7 \times 10^{-9}$ ) and SmBiT(78) ( $K_D = 3.4 \times 10^{-9}$ ).<sup>12</sup> Because of its small size, SmBiT was chosen for fusion to our POIs rhod and NCAM. LgBiT was successfully produced in *E. coli* (Figure S3). Analysis of POI

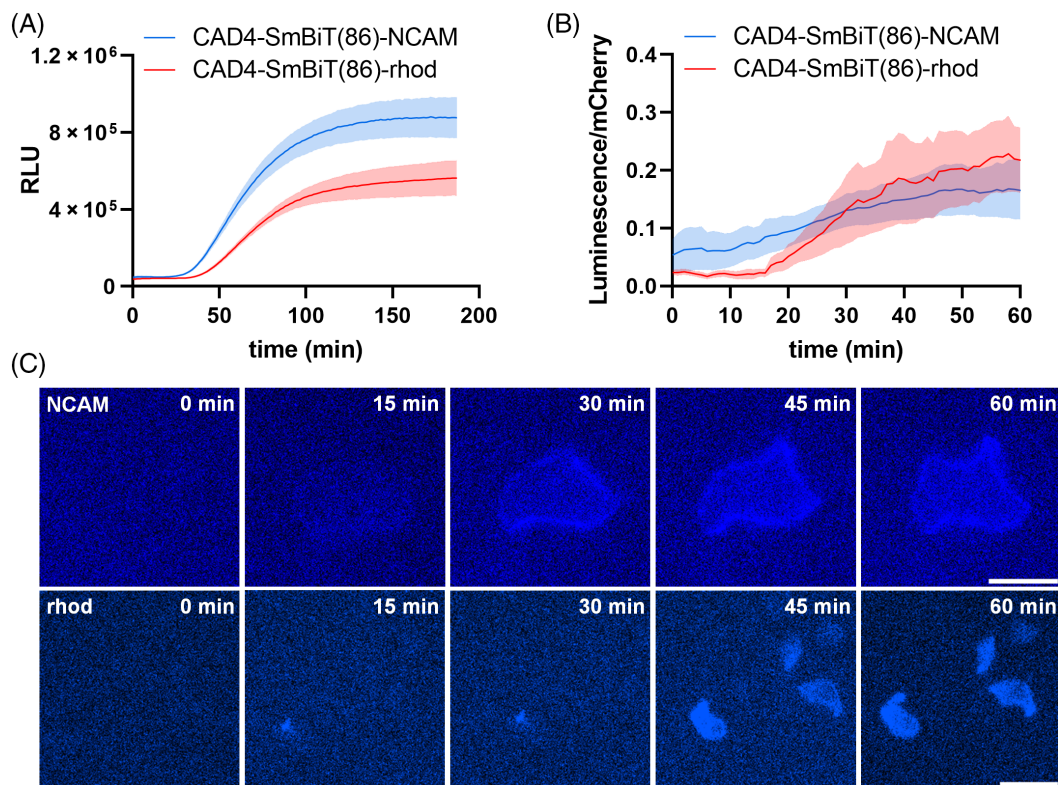


**FIGURE 4** Real-time detection of protein plasma membrane arrival. (A) Plate reader measurements of unpolarized MDCK cells that were transfected with the indicated construct 12 h prior to the experiment. LgBiT was added at 83.3 nM concentration and substrate was used in 1:300 dilution. Mean values of each time point of three time courses  $\pm$  SD are plotted. (B) Quantitative analysis of real-time microscopy data of the plasma membrane arrival of NCAM ( $N = 5$ ) and rhod ( $N = 12$ ). Luminescence values were normalized with mCherry signal. Mean values of each time point  $\pm$  SEM are plotted. (C) Representative images of selected time points for NCAM or rhod arrival at the plasma membrane. Images were acquired either with a  $60\times$  (NCAM, scale bar:  $20\ \mu\text{m}$ ) or a  $20\times$  (rhod, scale bar  $50\ \mu\text{m}$ ) objective.

localization by fluorescence microscopy before and after CAD release showed that SmBiT-tagged rhod and NCAM were not retained in the cytoplasm (Figure S4). Although SmBiT-tagged p75 was on average not significantly retained in the cytoplasm (Figure S4A, right panel), we saw that especially strongly expressing cells showed marked retention of p75 in the cytoplasm (see e.g., Figure S4A, left panel, condition 3 h release, AP). To avoid a potential bias because of such high expressing cells in bulk experiments with p75, we decided to use only NCAM and rhod as cargo for further experiments.

In the next step, we tested whether we could detect the three SmBiT variants at the cell surface. To do so, we used constructs without the CADs (SmBiT-HA-POI-mCherry), for the POIs to be constantly present at the plasma membrane without the addition of the D/D-Solubilizer. We could detect both rhod and NCAM using the low-affinity SmBiT(114) (Figure 3A,B). Luminescence signals only slightly increased 2.8-fold and 1.9-fold, respectively, for rhod and NCAM, compared to the LgBiT background signal. Using the high-affinity variants SmBiT(86) and SmBiT(78), fold-changes dramatically increased up to 6303-fold for rhod and 3441-fold for NCAM (Figure 3A,B). This high sensitivity and dynamic range of the system opens the possibility to detect even low protein amounts at the plasma membrane and enables luminescence detection at the single-

cell level with a microscope (Figure 3C). Higher LgBiT concentrations helped to achieve higher signal-to-noise ratios (Figure 3C, Figure S5A,B) and we verified a positive correlation between the protein amount (mCherry signal) and the luminescence intensity (Figure S5C,D).

### 2.3 | Real-time detection of plasma membrane arrival

After the successful detection of SmBiT-tagged proteins that were stably expressed at the plasma membrane, we moved on to measure the dynamic arrival of trafficked proteins at the cell surface. To do so, we transiently expressed the CAD constructs for rhod and NCAM in polarized MDCK cells and added D/D-Solubilizer simultaneously with LgBiT and substrate to the cells. Luminescence signals were then measured every minute in a plate reader. We could detect the arrival of the first proteins after  $\approx 30$  min followed by the wave of the other synchronously trafficked proteins. The signal saturated after  $\approx 120$  min, indicating that all proteins had arrived at the plasma membrane (Figure 4, Figure S6A). SmBiT(78) worked in a similar manner, whereas for SmBiT(114) signal changes were barely detectable,

pointing out the importance of a high affinity between LgBiT and SmBiT for spontaneous interaction and thereby providing a highly sensitive means for the detection of protein surface arrival (Figure S6A,B).

A typical problem with long luciferase measurements is the loss of substrate activity because of instability or degradation of enzymes over time. To distinguish whether signal decay after reaching the plateau derived from an actual change of protein amount, for example, because of protein internalization, or simply from loss of substrate activity, we made control measurements for each experiment (Figure S6C). To control for these effects, we expressed the respective constructs without the CADs and fixed the cells. In these controls, signal changes should have occurred exclusively because of changes in substrate activity. We used this data to normalize our protein arrival curves (Figure S6D).

Next, we confirmed our plate reader data by monitoring protein arrival at the plasma membrane in real time by microscopy. We recorded time series over 60 min and could show the arrival of rhod and NCAM at the plasma membrane (Figure 4B, Figure S7). The spatial resolution was high enough to see a characteristic plasma membrane signal for NCAM, which corresponds to the signal distribution that is expected to be seen in a microscopic z-section of a basolateral protein like NCAM (Figure 4C). These recordings open up entirely new possibilities for the spatial and temporal detection of protein plasma membrane arrival at single cell level. To ensure that the detected signal increase is indeed because of protein arrival at the plasma membrane, we inhibited protein trafficking using increasing concentrations of Brefeldin A (BFA), an inhibitor that blocks trafficking between the ER and the Golgi apparatus. First, we tested the constructs without CADs, and indeed luminescence signals decreased with increasing BFA concentrations for both, NCAM and rhod (Figure S8A,B). In line with this, synchronized cell surface arrival of CAD-SmBiT(86)-NCAM and CAD-SmBiT(86)-rhod after D/D-Solubilizer addition was impaired as well by BFA treatment (Figure S8C,D). Fluorescence microscopy analysis confirmed the enhanced retention of the POIs at the cytoplasm after BFA treatment (Figure S8E).

Furthermore, for comparison, we carried out experiments in which we added Alexa647-conjugated anti-HA antibodies to the medium of cells transfected with CAD-SmBiT(86)-NCAM or CAD-SmBiT(86)-rhod and imaged them during release with a confocal microscope to suppress out-of-focus signals from unbound anti-HA antibodies (Figure S9). Although this approach allowed for imaging surface arrival, we had to search for strongly expressing cells to detect surface signals that are clearly visible above the background of anti-HA antibodies in the medium.

## 2.4 | Specific detection of apical and basolateral protein arrival

Finally, we wanted to test if our system is capable of specifically distinguishing protein arrival at the apical and basolateral plasma

membrane. Therefore, we grew MDCK cells on the bottom of transwell filters until they formed a continuous polarized monolayer and transfected them with the constructs without the CADs. LgBiT and substrate were then added either to the apical or the basolateral side of the cell layers for polarity-specific detection (Figure S10). For NCAM, signals were only detectable if substrate and LgBiT were added to the basolateral side of the cells (Figure 5A), and for rhod it was vice versa (Figure 5B). With this experiment, we could show that our system based on split Nanoluciferase is able to detect the cell surface polarity of apical and basolateral membrane proteins precisely and quantitatively.

## 3 | DISCUSSION

Maintaining the concentration of cell surface proteins within tight boundaries is crucial for the proper function of a cell within a multicellular organism. However, directly measuring the cell surface concentration of a particular POI in live cells in real-time represents a considerable challenge. Here, we introduce an approach based on split luciferases and characterize it by biochemical and cell biological methods and demonstrate its applicability by using it to measure the cell surface arrival of CAD-synchronized proteins.

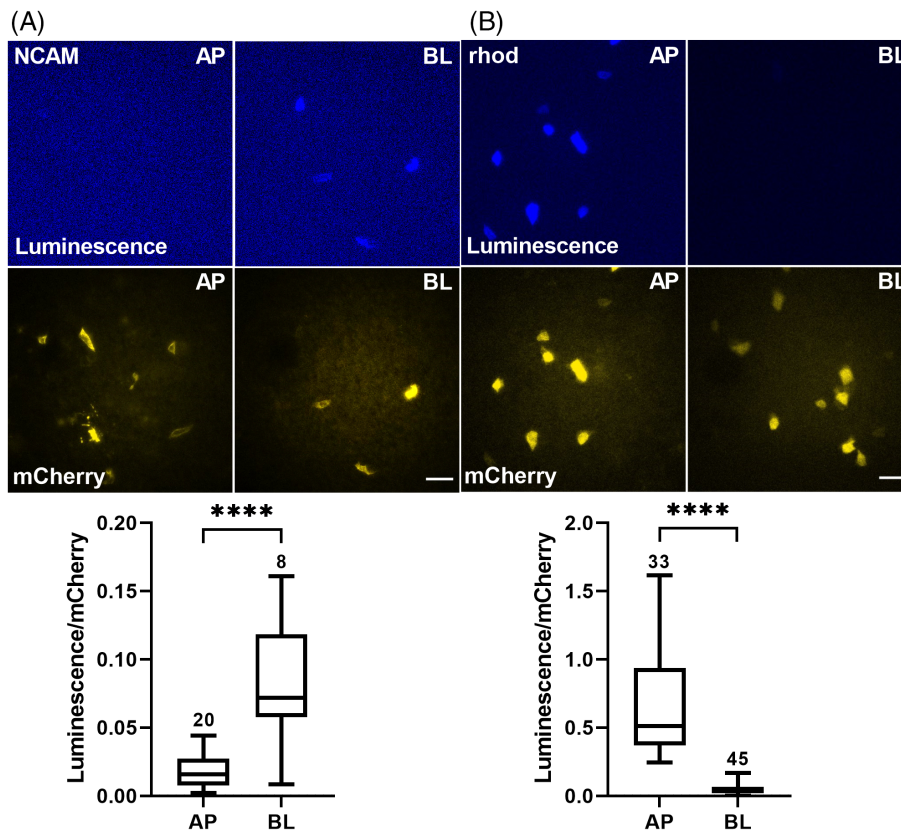
### 3.1 | Comparison of the utility of split Gaussia luciferase and split Nanoluciferase for real-time protein cell surface arrival assays

In our initial trials, we used split Gaussia luciferase including its “Monsta” variant. However, our experiments showed that split Gaussia luciferase does not have favorable properties for using it in split luciferase cell surface arrival assays. First, the signals after recombining split Gaussia luciferase were not high enough to enable sensitive measurements on a single-cell level. Second, a rather large fragment of split Gaussia luciferase needed to be attached to the POI, which often resulted in side effects on the natural trafficking of the POI. In comparison, split Nanoluciferase showed much higher signals after recombination. We measured a more than 6000-fold signal increase above the background. For reasonable POI expression levels, the total signal increase value is currently limited by the fact that the purified large fragment of split Nanoluciferase showed slight luminescence activity even without the presence of the small fragment. This could be because of other small peptides present in the extracellular medium, but the exact reason for this remains unknown.

### 3.2 | Applicability of our approach for studying polarized membrane trafficking in epithelial cells

We showed that our method can be used to monitor the polar cell surface arrival of apical and basolateral plasma membrane proteins in polarized epithelial cells. As we also demonstrated, the sensitivity of

**FIGURE 5** Apico-basal polarity-specific detection of NCAM and rhod. (A,B) Representative images and quantitative analysis of MDCK cells expressing SmBiT(86)-NCAM or SmBiT(86)-rhod constitutively at the plasma membrane. Cells were grown on the bottom of transwell filters until they formed a polarized monolayer. 3  $\mu$ M LgBiT and substrate diluted 1:100 in PBS were added apically or basolaterally directly prior measurement. NCAM images were acquired with 100 ms exposure time for mCherry and 2 s for luminescence. Three positions were acquired for both, basolateral and apical LgBiT addition. For rhod, 50 ms exposure time was used for mCherry and 1 sec for luminescence. Four positions were acquired for both, basolateral and apical LgBiT addition, scale bars indicate 50  $\mu$ m. For analysis, background signals were subtracted, and the luminescence signal was normalized with mCherry signal of each cell. *N* is indicated above each boxplot; *p* value was calculated with Student's *t* test (\*\*\*\**p* < 0.0001).



our system is sufficient to use it for single-cell experiments with a microscopic readout. This opens a multitude of novel possibilities. Classic methods to characterize protein sorting and polarized cell surface arrival in epithelial cells are based on biochemical readouts and utilize immunoprecipitation to measure radioactively pulse-chase labeled proteins and/or proteins that are labeled at the cell surface with reactive NHS-esters.<sup>17,19</sup> These biochemical methods are bulk measurements, usually from several million cells, and are therefore very sensitive to minor changes of the mean value but are not able to determine single-cell data. Thus, if two or more populations, which behave differently, are present in a sample, biochemical methods would mask this and just determine a mean overall populations. With our luciferase-based approach, bulk measurements using a plate reader as well as single-cell measurements using a microscope are possible, thus bringing the advantages of bulk and single-cell measurements together.

Virtually all data available on proteins or mutations that are relevant for polarized apical or basolateral protein sorting, are endpoint-measurements and/or bulk averages, and therefore might hide or “average out” several intricacies and/or sub-states during the sorting process. With the new split luciferase-based approach presented here, it will become possible to characterize and study these variations in single cells over time. It will be an interesting future endeavor to correlate the observed trafficking variations with variations in the expression and activity of sorting protein complexes at a single-cell level. We carried out antibody-based assays in previous studies<sup>5,13</sup> and clearly saw that cell surface arrival varies significantly

between individual cells, thus suggesting that these variations matter.

An alternative method to detect POI cell surface arrival is applying antibodies to the extracellular medium. This allows to read out the cell surface concentration of POIs at the individual cell level. As we showed here, antibody-based methods can be used for live cell real-time measurements. However, unbound antibodies created background signals, even if a confocal microscope was used to diminish out-of-focus signals. Thus, real-time imaging of POI cell surface arrival using extracellular antibodies was limited to cells expressing the POI at sufficiently high levels, because in low-expressing cells, the surface signal was not significantly higher than the background signal level. Furthermore, for long-term imaging and/or imaging at high repetition rates, bleaching of the fluorophore will become an issue. To achieve a higher signal-to-noise with antibody-based methods for POI cell surface detection, the antibodies can be washed out. However, this limits the achievable time resolution. Another alternative is the usage of fluorogenic probes that only produce signal when they are bound to the POI and thus reduce background signal levels. Fluorogenic probes for detecting POI cell surface arrival have been already described.<sup>6</sup> Currently, the sensitivity of fluorogenic probe-based approaches is limited because the probes produce only a six-fold increase of fluorescence signal levels upon binding. It will be interesting to see in the future how probes with higher fluorogenic increase can be adapted and utilized for detecting the cell surface arrival of POIs.

Because the luciferase substrate used for the split Nanoluc-tagged system, furimazine, is membrane permeable, also POI-SmBiT-LgBiT-conjugates that assembled at the cell surface and

are subsequently endocytosed, will keep producing luminescence signals. In this sense, the readouts we measured here represent the integrated number of POIs that arrived at the cell surface over the time LgBiT was added to the medium. This characteristic of our approach would make it difficult to measure the amount of cell surface arrival in case of constitutively expressed and trafficked POIs. For constitutive membrane proteins, a large amount is already present at the cell surface at the beginning of the measurement. This would produce high luminescence signals, which would only slightly change by the typically low rate of newly arriving proteins at the cell surface. However, blocking a cohort of surface POIs could be achieved by designing a non-active mutant of LgBiT or a SmBiT-specific antibody that occupies all POIs at the cell surface at the beginning of the measurement. LgBiT that is added after this blocking step will only bind to, and thus detect, newly arriving SmBiT-tagged membrane proteins.

### 3.3 | Potential further applications of the split luciferase-based approach for detecting the cell surface arrival of proteins

The split luciferase approach presented here could also be used for detecting the release of soluble proteins from cells, especially when a plate reader is used as readout modality. Furthermore, our approach will be also applicable to detect regulated exocytosis or secretion of proteins. One disadvantage of our approach is that a tag at an extracellular domain of the POI is required. Although this tag, SmBiT, is rather small (only a 11 amino acids), which makes interference with the natural function of the POI less likely, there will be POIs for which attaching even a small tag at the extracellular side of the POI is not feasible.

We expect that split luciferase-based approaches are well suited for long-term measurements in cells, because no fluorescence excitation is required and thus no resulting phototoxic effects are produced. Nevertheless, it is possible to combine fluorescent readouts with luminescence readouts, thus enhancing the number of parameters that can be probed during an experiment.

The split luciferase-based approach described here would even make it possible to carry out measurements of protein surface arrival in more complex model systems, such as organoids, provided a sufficiently membrane-permeable luciferase substrate is used. To fill closed lumina within organoids with LgBiT, it could be injected into lumina. Alternatively, a construct enabling to fill lumina by regulated expression and secretion of LgBiT before start of the measurement could be transfected. Furthermore, the split-luciferase approach could also be used to detect transcytosis across epithelia and endothelia.

## 4 | MATERIALS AND METHODS

### 4.1 | DNA cloning and production

Plasmids were cloned by restriction enzyme cloning or Gibson assembly.<sup>20</sup> Short DNA fragments up to 80 bp were inserted by aligning

two compatible primers (Merck KGaA) that mimic specific restriction enzyme sites at both ends. The alignment was achieved by mixing 20  $\mu$ L of each forward and reverse primer (100  $\mu$ M) with 20  $\mu$ L 20 M NaCl-solution and 20  $\mu$ L H<sub>2</sub>O and heating to 95°C for 10 min. The mix was slowly cooled down to room temperature, diluted 1:100 and used for the ligation using the Quick Ligation Kit (New England Biolabs). Specific base pair substitutions were introduced with site-directed mutagenesis by polymerase chain reaction (PCR). Sequences were verified by Sanger sequencing. All used plasmids are listed in Table S1.

### 4.2 | Recombinant protein production and purification

Recombinant luciferase fragments were produced in *E. coli* BL21 (DE3). 1 L bacterial cultures were grown at 37°C, 150 rpm in LB-Medium (Roth). Upon reaching OD<sub>600</sub> = 0.6–0.8, the expression was induced with 1 mM isopropyl  $\beta$ -D-1-thiogalactopyranoside (IPTG). The expression was sustained for 20–24 h at 18°C and 150 rpm. Cultures were harvested by centrifugation (6000g, 10 min) and pellets were resuspended in 30 mL nickel (Ni)-lysis buffer (50 mM NaH<sub>2</sub>PO<sub>4</sub>  $\times$  2 H<sub>2</sub>O, 300 mM NaCl, 1 mM Imidazole, pH 8). Lysates were shock frozen in liquid nitrogen and stored at –80°C. Recombinant proteins were purified over nickel-nitrilotriacetic acid (Ni-NTA) Agarose (Qiagen). Therefore, lysates were thawed in a water bath at 37°C, sonicated (Bandelin Sonoplus HD 3100 homogenizer) for 10 min at 60% amplitude on ice and centrifuged for 1 h with 30.000g at 4°C. Polypropylene gravity-flow columns (Thermo Fisher) were prepared with 1 mL Ni-NTA Agarose according to the manufacturers protocol and equilibrated twice with 15 mL Ni-lysis buffer. Cleared lysates were added to the columns and subsequently washed twice with 15 mL Ni-wash buffer (50 mM NaH<sub>2</sub>PO<sub>4</sub>  $\times$  2 H<sub>2</sub>O, 300 mM NaCl, 20 mM Imidazole, pH 8). Elution with Ni-Elution Buffer (50 mM NaH<sub>2</sub>PO<sub>4</sub>  $\times$  2 H<sub>2</sub>O, 300 mM NaCl, 250 mM Imidazole, pH 8) was done in 1 mL steps. Protein content was confirmed by mixing 2  $\mu$ L of each elution step with 200  $\mu$ L Bradford solution (Protein assay dye reagent (Bio-Rad) diluted 1:5 in H<sub>2</sub>O). Eluates containing protein were pooled and analyzed via SDS-PAGE and coomassie brilliant blue staining. Protein concentration was determined via Bradford protein assay and adjusted to 0.1 mg/mL in phosphate-buffered saline (PBS) containing calcium, magnesium (PBS (+/+), Life Technologies) and 0.1% glycerol to be stored in aliquots at –80°C.

### 4.3 | Mammalian cell culture and transfection

Madin-Darby Canine Kidney cells subclone II (MDCK II, kindly provided by Enrique Rodriguez-Boulan, Weill Cornell Medical College) were cultivated at 37°C and 5% CO<sub>2</sub> in Dulbecco's Modified Eagle Medium (DMEM, Life Technologies) containing 5% fetal calf serum (FCS, Life Technologies) and 2 mM L-glutamine. Cells were passaged after reaching a confluency of 80%–90%. For experiments, cells were



seeded onto assay plates and transfected using polyethylenimine (PEI, Polyscience, 1 mg/mL). Details on the conditions for each experiment can be found in Table S2.

#### 4.4 | Generation of stable cell lines

To generate stable cell lines,  $2.5 \times 10^5$  cells were seeded on a 6-well plate. The next day they were transfected with the desired vector, containing a resistance to geneticin (G418). After overnight incubation, cells were detached from the plate, diluted 1:10, 1:20, 1:50 and 1:200 with DMEM containing 5  $\mu$ g/mL G418 (Roth) and seeded on 10 cm dishes. Cells were then grown for approximately 2 weeks until single colonies were grown. The medium was refreshed twice a week. Single colonies were isolated and mCherry-positive colonies were selected by confocal microscopy.

#### 4.5 | Luciferase experiments using a plate reader

Luciferase experiments in 96-well format were measured using a Tecan Infinite M200 Pro or an BioTek Instruments Synergy 4 multi-mode microplate reader. All measurements were performed in triplicates in white, flat-bottomed 96-well plates after 1 min shaking and with an integration time of 1000 ms. Substrate was always prepared freshly, protected from light and added directly prior the measurement. For the Gaussia luciferase, 100  $\mu$ L injections of coelenterazine (Roth, 20  $\mu$ M, in PBS) were used and for the Nanoluciferase, 50  $\mu$ L injections of Furimazine (Nano-Glo<sup>®</sup> Luciferase Assay Substrate, Promega) were applied. The substrate was diluted 1:50 in Nano-Glo<sup>®</sup> Luciferase Assay Buffer for recombinant proteins or in PBS for luminescence measurement in cells. Recombinant luciferase fragments were always thawed freshly for each experiment, combined in the desired concentrations and measured at room temperature. To detect luciferase fragments on the surface of cells, stable cell lines or cells to be transfected 24 h prior the measurement were seeded onto tissue culture-coated, white 96-well plates 48 h prior the experiment.

For control experiments in which the steady amount of luciferase fragments at the surface was measured, cells were fixed with 4% paraformaldehyde solution (PFA) for 15 min at room temperature, washed with PBS and remaining PFA was quenched with 50 mM  $\text{NH}_4\text{Cl}$  for 2 min at room temperature. Afterwards, the respective other recombinant fragment of the split luciferase was added to the desired concentration.

For inhibition of trafficking with BFA (eBioscience<sup>™</sup>, ThermoFisher Scientific) in cells expressing constructs without CAD-domains, medium was changed 8 h after transfection with medium containing the concentrations of BFA that are indicated in the figures. Cells were incubated for 15 h and then washed with PBS. LgBiT (83.3 nM) and Furimazine (1:300) were added and luminescence was measured immediately.

To detect protein arrival at the cell surface in cells expressing constructs with CAD-domains, cells were washed with PBS, then LgBiT (83.3 nM) was added. D/D-Solubilizer (5  $\mu$ M) without cycloheximide

was mixed with the substrate (1:300) and added directly prior to the measurement. For experiments in which protein trafficking was inhibited with BFA, cells were preincubated for 4 h with the indicated concentrations of BFA diluted in DMEM. Then DMEM was replaced by PBS containing LgBiT, substrate and the same BFA concentration as before. Cells were preincubated for 15 min with this mix, then D/D-Solubilizer was added and the measurement was started. In all cases, protein surface arrival was measured at 37°C and the arrival curves were corrected for the loss of substrate activity by normalization to the control samples (Figure S6).

#### 4.6 | Sample preparation for microscopy

For synchronized release microscopy experiments with polarized cells, MDCK II cells were seeded on transwell filters (#3401, Corning-Costar) and grown for 4 days. The medium was changed daily. Eight hours after transfection, cells were incubated with D/D-Solubilizer (5  $\mu$ M, Clonetech/Takara) and cycloheximide (35.54  $\mu$ M, Merck) for 3 h at 37°C for releasing a synchronized wave of proteins from the ER. To detect HA-tagged proteins at the cell surface, a HA-Cy5-antibody (mouse anti-HA antibody [Covance, PRB-101C]), conjugated to Cy5 using a Cy5 conjugation kit (GE Healthcare) was diluted 1:500 in medium and applied to the apical or basolateral side of the transwell filters. After 15 min incubation at 37°C, cells were washed twice with PBS, fixed with 4% PFA for 15 min at room temperature and washed again with PBS. Staining of nuclei was performed by incubating the samples for 30 min with 1  $\mu$ g/mL DAPI (Thermo Fisher Scientific) in SAPO solution (0.02% saponin, 0.2% BSA in PBS). Samples were washed three times with PBS. Coverslips were mounted in 8.5  $\mu$ L Mowiol mounting medium (200% Tris HCl [0.2 mM, pH 8.5], 100% Glycerol, 40% Mowiol [Roth] in  $\text{H}_2\text{O}$ ), supplied with 1,4-Diazabicyclo[2.2.2]octan-medium (Dabco-medium, Tris HCl (50 mM, pH 8), 2.5% Dabco (Merck) in glycerol), whereas transwell filters were excised and mounted in Dabco-medium.

Live cell imaging was performed in live cell imaging chambers (Ibidi) or on transwell filters. To enable imaging with transwell filters, the cells were seeded onto the downside of transwell filters. To do so, the transwell inserts were placed bottom-up on a 10 cm dish and 400  $\mu$ L cell suspension was added. The dish was then carefully covered with the lid, without destroying the drop of cell suspension and incubated for 3 h until the cells were attached to the filter. Then the filters were transferred back into a 12-well plate and covered with medium. In order to grow a tight and intact monolayer, the medium was changed every day for 7 days. For transfection, the transwell filters were again placed bottom up on a 10 cm dish, the transfection mix was applied and incubated for 6–8 h at 37°C. The filters were then transferred back into the 12-well plate and incubated overnight. Directly before imaging, the filters were carefully placed on a 32 mm live cell imaging chamber with 750  $\mu$ L PBS or DMEM without phenol red (Figure S10). For the experiment, PBS or DMEM was replaced by the respective recombinant luciferase fragment that was mixed with the substrate and added either apically or basolaterally.

## 4.7 | Imaging and image analysis

Fluorescent images were acquired using a Nikon Eclipse Ti.E A1R inverted confocal laser scanning microscope equipped with a 60X oil immersion objective (numerical aperture (N.A.) = 1.49) and lasers emitting at 405, 488, 561 and 641 nm. To measure the polarity of cell surface arrival (labeled as “sorting efficiency” in graphs), z-stacks covering the complete cell height were recorded and cells were analyzed using a custom-written Matlab program as described before.<sup>5,13,21</sup> To measure the percentage of proteins that reached the cell surface (labeled as “% surface protein” in graphs), the Manders' fractional overlap coefficient (M) between the surface signals (S) from anti-HA staining and the total protein signals (T) from mCherry-tags was calculated. To this end, thresholds ( $th_S$  and  $th_T$ , respectively) were manually set for the S and T channels to exclude background signals. Then, M was calculated according to the formula  $M = \sum_i T_{i,colocal} / \sum_i T_i$  where  $T_{i,colocal} = T_i$  if  $S_i > 0$  and  $T_{i,colocal} = 0$  otherwise with the index  $i$  running over all voxels in the z-stack. Luciferase signals were imaged by combining the A1R confocal setup with an ANDOR DU-897 EMCCD camera and a 20 $\times$  plan apochromatic objective (N.A. = 0.75). To detect the full luminescence spectrum, no filter cube was used. For image analysis, the background was subtracted, and luminescence signals were normalized to mCherry signals. For time series, several positions on the sample were chosen, and one picture per minute was recorded over a period of 2–3 h.

### ACKNOWLEDGMENTS

Roland Thuenauer acknowledges support from the Ministry of Science, Research and the Arts of Baden-Württemberg (project: Split luciferase-mediated detection of trafficked protein localization). This work was further supported by the German Research Foundation (Deutsche Forschungsgemeinschaft, DFG) under Germany's Excellence Strategy—CIBSS, EXC-2189, Project ID: 390939984 and in part by the Ministry for Science, Research and Arts of the State of Baden-Württemberg (Az: 33-7532.20). Open Access funding enabled and organized by Projekt DEAL.

### CONFLICT OF INTEREST STATEMENT

All authors declare that they have no conflicts of interest.

### PEER REVIEW

The peer review history for this article is available at <https://www.webofscience.com/api/gateway/wos/peer-review/10.1111/tra.12908>.

### DATA AVAILABILITY STATEMENT

Data are available upon request from the corresponding author.

### ORCID

Alexandra A. M. Fischer  <https://orcid.org/0000-0001-9628-0534>

Roland Thuenauer  <https://orcid.org/0000-0002-5369-1699>

### REFERENCES

1. Farhan H, Rabouille C. Signalling to and from the secretory pathway. *J Cell Sci.* 2011;124:171-180.

2. Royle SJ, Murrell-Lagnado RD. Constitutive cycling: a general mechanism to regulate cell surface proteins. *Bioessays.* 2003;25:39-46.
3. Rodriguez-Boulan E, Macara IG. Organization and execution of the epithelial polarity programme. *Nat Rev Mol Cell Biol.* 2014;15:225-242.
4. Cossarizza A, Chang HD, Radbruch A, et al. Guidelines for the use of flow cytometry and cell sorting in immunological studies (third edition). *Eur J Immunol.* 2021;51:2708-3145.
5. Stroukov W, Rösch A, Schwan C, Jeney A, Römer W, Thuenauer R. Synchronizing protein traffic to the primary cilium. *Front Genet.* 2019;10:163.
6. Jonker CTH, Deo C, Zager PJ, et al. Accurate measurement of fast endocytic recycling kinetics in real time. *J Cell Sci.* 2020;133:jcs231225.
7. Leng S, Qiao Q, Miao L, Deng W, Cui J, Xu Z. A wash-free SNAP-tag fluorogenic probe based on the additive effects of quencher release and environmental sensitivity. *Chem Commun.* 2017;53:6448-6451.
8. Pedelacq J-D, Cabantous S. Development and applications of superfolder and split fluorescent protein detection systems in biology. *Int J Mol Sci.* 2019;20:3479.
9. Romei MG, Boxer SG. Split green fluorescent proteins: scope, limitations, and outlook. *Annu Rev Biophys.* 2019;48:19-44.
10. Tebo AG, Gautier A. A split fluorescent reporter with rapid and reversible complementation. *Nat Commun.* 2019;10:1-8.
11. Remy I, Michnick SW. A highly sensitive protein-protein interaction assay based on Gaussia luciferase. *Nat Methods.* 2006;3:977-979.
12. Dixon AS, Schwinn MK, Hall MP, et al. NanoLuc complementation reporter optimized for accurate measurement of protein interactions in cells. *ACS Chem Biol.* 2016;11:400-408.
13. Thuenauer R, Hsu YC, Carvajal-Gonzalez JM, et al. Four-dimensional live imaging of apical biosynthetic trafficking reveals a post-Golgi sorting role of apical endosomal intermediates. *Proc Natl Acad Sci U S A.* 2014;111:4127-4132.
14. Thuenauer R, Nicklaus S, Frensch M, Troendle K, Madl J, Römer W. A microfluidic biochip for locally confined stimulation of cells within an epithelial monolayer. *RSC Adv.* 2018;8:7839-7846.
15. Thuenauer R, Juhasz K, Mayr R, et al. A PDMS-based biochip with integrated sub-micrometre position control for TIRF microscopy of the apical cell membrane. *Lab Chip.* 2011;11:3064-3071.
16. Youker RT, Bruns JR, Costa SA, et al. Multiple motifs regulate apical sorting of p75 via a mechanism that involves dimerization and higher-order oligomerization. *Mol Biol Cell.* 2013;24:1996-2007.
17. Deborde S, Perret E, Gravotta D, et al. Clathrin is a key regulator of basolateral polarity. *Nature.* 2008;452:719-723.
18. Kim SB, Suzuki H, Sato M, Tao H. Superluminescent variants of marine luciferases for bioassays. *Anal Chem.* 2011;83:8732-8740.
19. Carvajal-Gonzalez JM, Gravotta D, Mattera R, et al. Basolateral sorting of the coxsackie and adenovirus receptor through interaction of a canonical YXX motif with the clathrin adaptors AP-1A and AP-1B. *Proc Natl Acad Sci.* 2012;109:3820-3825.
20. Gibson DG, Young L, Chuang R-Y, Venter JC, Hutchison CA, Smith HO. Enzymatic assembly of DNA molecules up to several hundred kilobases. *Nat Methods.* 2009;6:343-345.
21. Müller SK, Wilhelm I, Schubert T, et al. Gb3-binding lectins as potential carriers for transcellular drug delivery. *Expert Opin Drug Deliv.* 2017;14:141-153.

### SUPPORTING INFORMATION

Additional supporting information can be found online in the Supporting Information section at the end of this article.

**How to cite this article:** Fischer AAM, Schatz L, Baaske J, Römer W, Weber W, Thuenauer R. Real-time monitoring of cell surface protein arrival with split luciferases. *Traffic.* 2023; 24(10):453-462. doi:10.1111/tra.12908